NASA TM X-1363

PENETRATION OF DROPS INTO HIGH-VELOCITY AIRSTREAMS

By Robert D. Ingebo

Lewis Research Center
Cleveland, Ohio

NATIONAL AERONAUTICS AND SPACE ADMINISTRATION

For sale by the Clearinghouse for Federal Scientific and Technical Information
Springfield, Virginia 22151 – CFSTI price $3.00

PENETRATION OF DROPS INTO HIGH-VELOCITY AIRSTREAMS

by Robert D. Ingebo

Lewis Research Center

SUMMARY

Drop penetration distances and drop sizes were determined experimentally for crosscurrent injection of isooctane jets into airstreams at a distance of 1 inch downstream from the injector orifice. The results were obtained by photographing the fuel spray with a high-speed camera, and measuring the fuel-air concentration in the spray by a sampling probe technique. Thus, it was possible to relate the maximum penetration distance of the spray to the maximum observed drop size and the ratio of the Reynolds and Weber numbers. Also the point of maximum fuel concentration in the spray was related to the volume-number mean drop diameter and the ratio of the Reynolds and Weber numbers.

Results were compared with other data in the literature and agreement was fairly good over a relatively wide range of airstream and liquid-jet injection conditions. In this study, the effect of airstream velocity proved to be considerably greater than the effect of the liquid-jet velocity on drop penetration and drop sizes.

INTRODUCTION

Methods of injecting a fuel into an oxidizing gas stream, such as that produced in a jet engine or a rocket combustor, fall into three main categories: gaseous, liquid, or slurry fuel-injection systems. The most generally used type, of course, is liquid injection, since it is relatively easy to break up liquids and the droplets thus formed penetrate farther into the gas stream than gaseous jets. The slurry fuels (solid-liquid combinations) also have a penetration advantage over gaseous jets.

The method used to inject liquid fuels into airstreams is important to the performance of jet engines (refs. 1 and 2). There is, however, a lack of knowledge of the effect of many of the factors important to the breakup process and the subsequent trajectory, acceleration, and vaporization of the drops on the combustion process.

This investigation was conducted to determine the drop-size distribution of sprays produced by the crosscurrent injection of a liquid jet into a high-velocity airstream and to determine the distance of penetration of the measured drops into the airstream. For

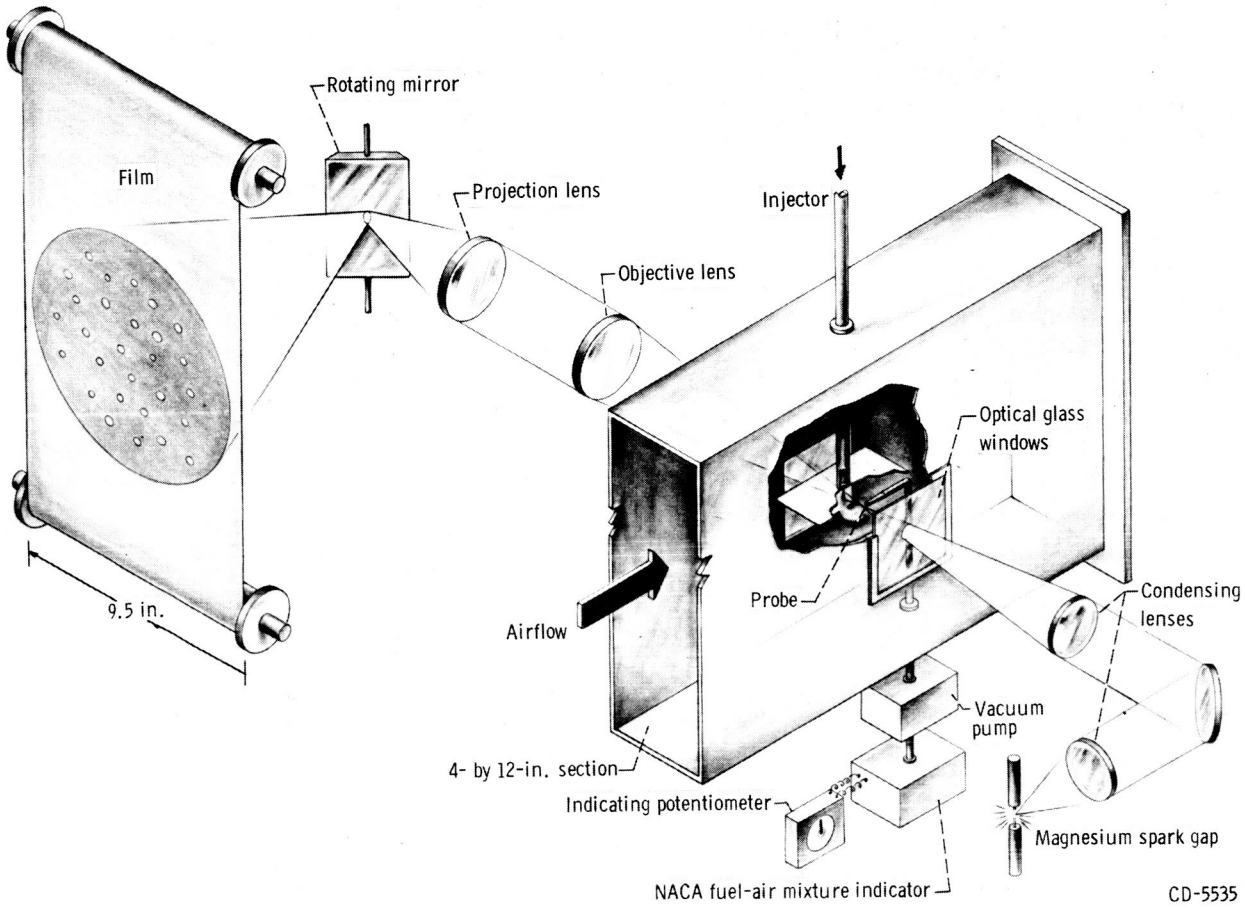

Figure 1. - Diagram of test section equipment and camera unit.

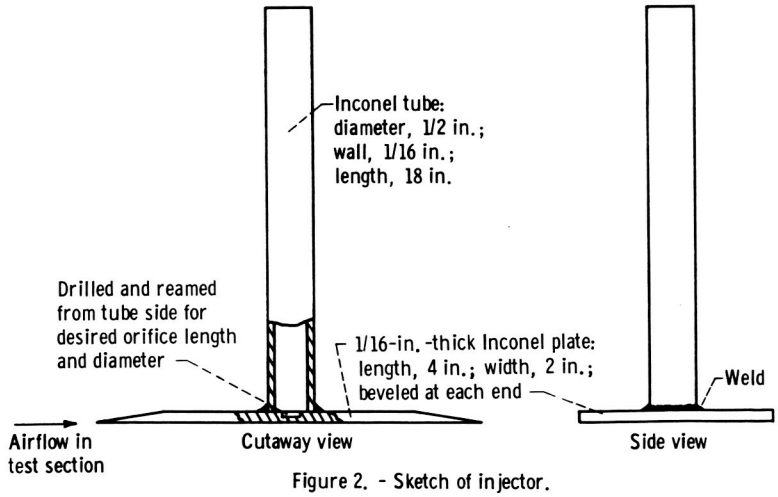

Figure 2. - Sketch of injector.

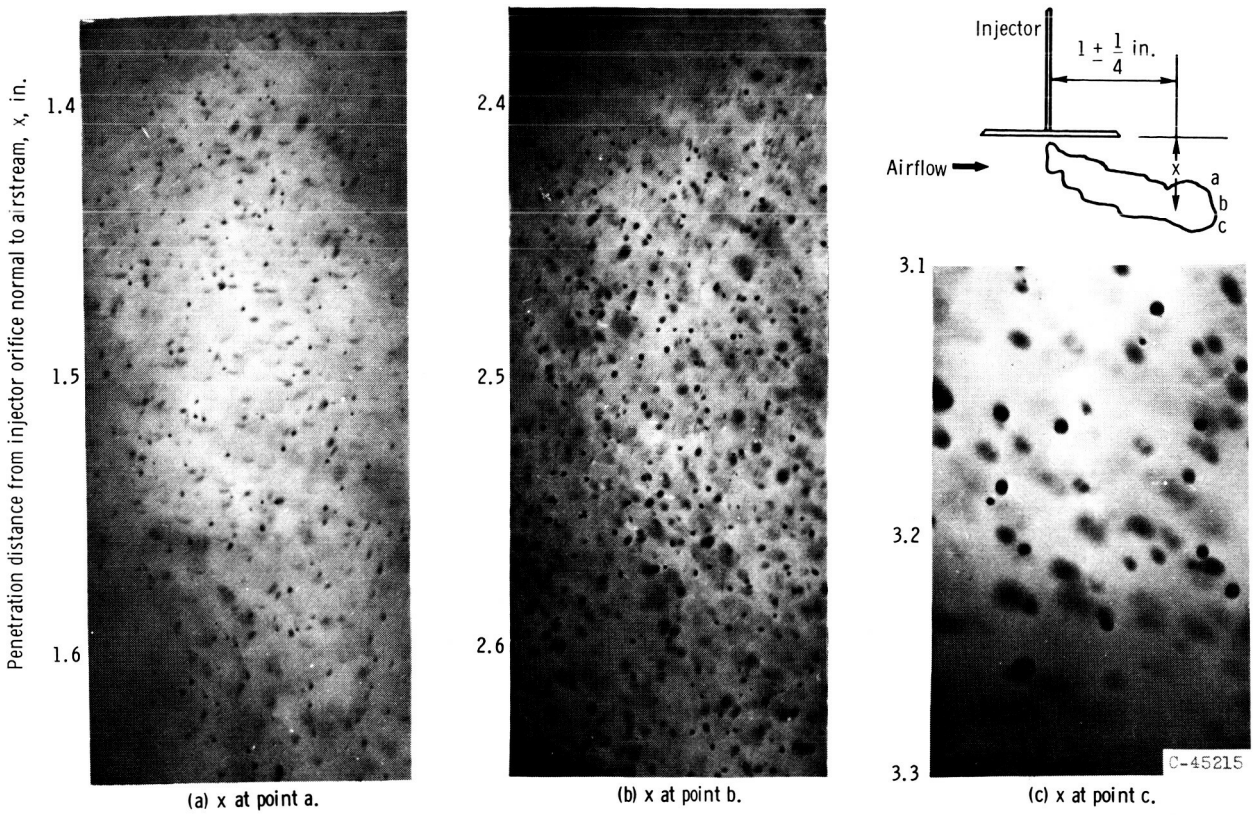

Figure 3. - Photomicrographs of isooctane spray in 100-feet-per-second-velocity airstream (data from table 1). Magnification, X21.

these purposes, a high-speed camera, capable of photographing microscopic droplets traveling at high velocities in airstreams (ref. 3), was used in combination with a sampling probe (ref. 4). From the data obtained with the high-speed camera and the sampling probe, it was possible to derive empirical expressions for the penetration distance of drops produced by crosscurrent injection of liquid-fuel jets into airstreams.

EXPERIMENTAL PROCEDURE

The equipment used in this study is shown in figure 1. Details of the injector are shown in figure 2. Isooctane (2, 2, 4-trimethylpentane) was injected through a simple orifice in a flat plate, with the liquid jet oriented normal to the airstream at the center of the test section.

The spray was photographed with a high-speed camera developed at the Lewis Research Center to track droplets accelerating and vaporizing in airstreams. Construction details of the camera have been previously reported (ref. 3). Drop-size-distribution data were obtained from photomicrographs of the sprays (fig. 3). The pictures were taken along a vertical traverse of the spray centerline, normal to the airstream, at a

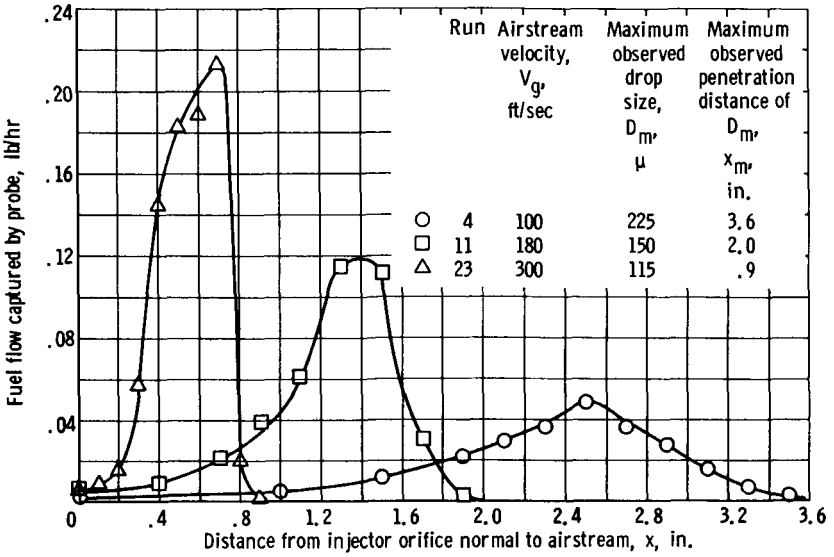

Figure 4. - Distribution of isoctane sprays normal to airflow and 1 inch downstream from injector. Orifice diameter, 0.030 inch; fuel jet velocity, 51 feet per second; fuel density, 42.6 pounds per cubic foot; air temperature, 86° F; air pressure, 29.3 inches of mercury, absolute.

TABLE I. - PENETRATION DISTANCES FOR CHARACTERISTIC DROP SIZES

Run	Orifice diameter, D_o, in.	Liquid-jet velocity, V_j, ft/sec	Airstream velocity, V_g, ft/sec	Maximum observed drop diameter, D_m, μ	Maximum observed penetration distance of D_m, x_m, in.	Volume-number mean drop, diameter, D_{30}, μ	Point of maximum fuel concentration, x_c, in., (a)	Penetration distance calculated from Chelko's equation (ref. 6), k	
								0.450	0.535
1	0.010	180	100	175	3.0	55	1.8	2.7	3.2
2	.020	81	↓	225	3.7	68	2.2	2.1	2.5
3	.020	80	↓	190	3.0	69	2.3	2.1	2.5
4	.030	51	↓	225	3.6	81	2.5	1.9	2.3
5	.030	76	180	175	3.2	65	2.2	2.0	2.4
6	.040	59	180	190	2.6	62	1.8	1.6	1.9
7	.020	80	180	150	1.9	47	1.0	1.3	1.5
8	↓	81	↓	140	1.8	47	1.2	1.3	1.5
9	↓	84	↓	150	1.8	49	1.2	1.3	1.5
10	↓	204	↓	140	3.2	47	2.1	2.9	3.5
11	.030	51	↓	150	2.0	52	1.4	1.2	1.4
23	.030	51	300	115	.9	40	.7	.7	.8

[a]Based on point of maximum fuel concentration in spray-profile data.

distance of $1\pm\frac{1}{4}$ inch downstream from the injector. Vertical traverses made at distances of 1 inch on either side of the spray centerline showed no measurable effect of horizontal displacement on drop-size distribution.

The sampling probe, described in reference 4, was used for continuous sampling of the spray, at the airstream velocity and on the same vertical traverse used for the camera. The isooctane and air mixtures captured by the probe were passed through a NASA fuel-air mixture analyzer. Results from this sampling technique gave the spray-concentration data shown in figure 4.

From spray-concentration data and drop-size-distribution data, the maximum observed penetration distance x_m and the maximum observed drop size D_m were readily determined. For example, in figure 4 the value of x_m was 3.6 inches for a maximum observed drop diameter of 225 microns and an airstream velocity of 100 feet per second. All the data obtained in these tests are given in table I; the run numbers correspond to those given in reference 5.

ANALYSIS

Photomicrographs, at a magnification of 21 times the drop diameter, were obtained as shown in figure 3 (p. 3). They indicate that a partial fractionation of the spray occurred in the atomization process because the large high-momentum drops penetrated farther into the airstream than the small low-momentum drops. Thus, in the momentum exchange process between the airstream and the drops, the penetration distance x for a given drop appears to be a function of the drop diameter D. Similarly, the maximum observed penetration distance x_m of the spray into an airstream might be assumed to be a function of the maximum drop diameter D_m.

Relation of Maximum Penetration Distance to Reynolds and Weber Numbers

In reference 5, the maximum drop diameter was found to be a function of the Reynolds and Weber numbers based on the orifice diameter D_o. Thus, the maximum observed penetration distance might also be assumed to be a function of the Reynolds and Weber numbers; that is,

$$\frac{x_m}{D_o} = f(Re, We) \tag{1}$$

when expressed in nondimensional form. Equation (1) may be rewritten as

$$\frac{x_m}{D_o} = a\left(\frac{D_o V_l \rho_l}{\mu_l}\right)^m \left(\frac{\rho_g D_o V_g^2}{\sigma}\right)^h \tag{2}$$

where a, m, and h are constants; V_l, ρ_l, μ_l, and σ are the liquid velocity, density, viscosity, and surface tension, respectively; and ρ_g and V_g are the gas density and velocity, respectively. Thus, x_m is assumed to be a function of the ratio of dynamic to viscous forces of the liquid, and also the ratio of the dynamic force of the airstream to the surface-tension force of the liquid.

The effect of Weber number on the maximum penetration distance was determined at relatively constant values of Reynolds number. From the plot of the data shown in figure 5, it appears that

$$\frac{D_m}{D_o} \propto We^{-0.7}$$

Thus, equation (2) may be rewritten as

$$\frac{x_m}{D_o} = a\, Re_l^m\, We^{-0.7} \tag{3}$$

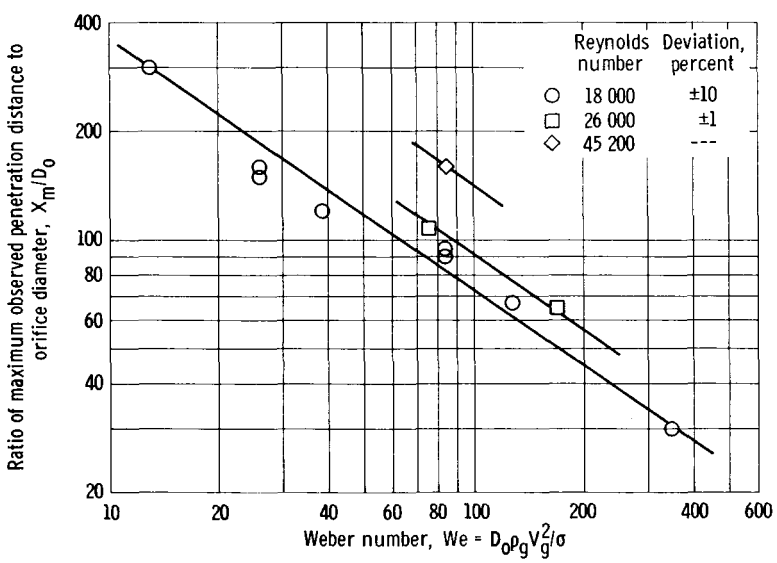

Figure 5. - Effect of Weber number on maximum penetration distance of spray.

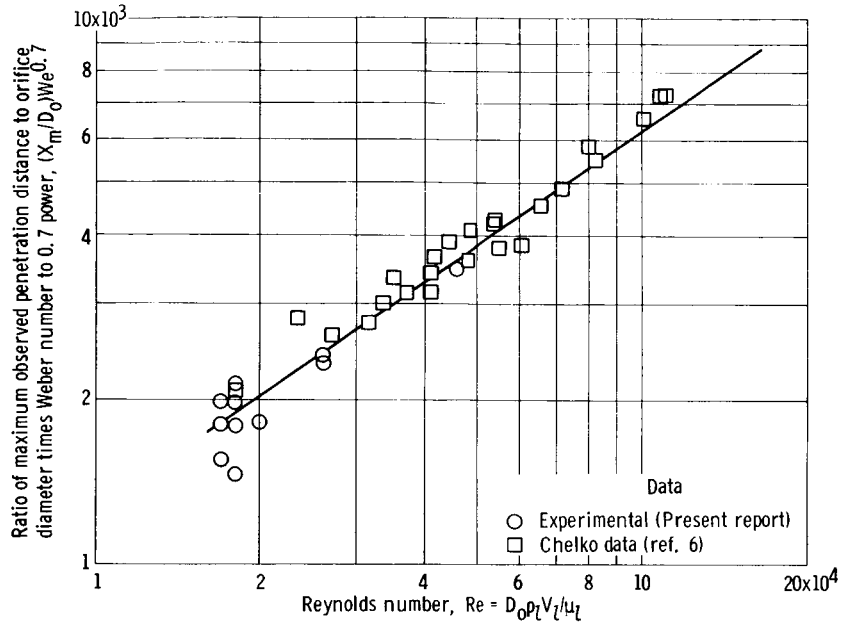

Figure 6. - Effect of Reynolds number on maximum penetration distance of spray with Chelko's data included.

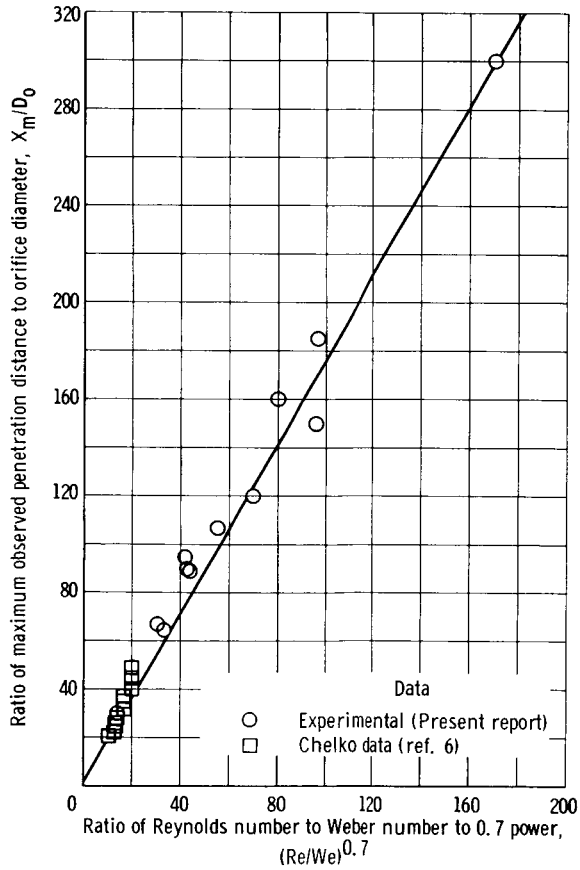

Figure 7. - Evaluation of constant a in equation (4).

To determine the effect of Reynolds number on the maximum observed penetration distance, $(x_m/D_o)\ We^{0.7}$ was plotted against Reynolds number, as shown in figure 6 (p. 7). The Reynolds number range was extended by including the data of Chelko, which indicate the same trend shown in this study. From the figure, it is evident that $x_m \propto Re^{0.7}$, and equation (3) may be rewritten as

$$\frac{x_m}{D_o} = a\left(\frac{Re}{We}\right)^{0.7} \tag{4}$$

The value of the constant a, as determined from figure 7 (p. 7), was 1.8. Thus, equation (4) becomes

$$\frac{x_m}{D_o} = 1.8\left(\frac{Re}{We}\right)^{0.7} \tag{5a}$$

This expression correlates the maximum observed penetration distance with the Reynolds and Weber numbers for both the data obtained in this study and that obtained by Chelko.

Equation (5a) may be written as

$$\frac{x_m}{D_o} = 1.8\left(\frac{q_l}{q_g}\frac{\sigma}{\mu_l V_l}\right)^{0.7} \tag{5b}$$

where $q_l = \frac{1}{2}\rho_l V_l^2$ and $q_g = \frac{1}{2}\rho_g V_g^2$. In this case, x_m/D_o is expressed as a function of the ratio of the dynamic pressure of the liquid jet to that of the airstream and the ratio of surface tension to viscous forces of the liquid.

Relation of Maximum Penetration Distance to Maximum Drop Diameter

Since both the maximum penetration distance and the maximum drop diameter appear to be related to the Reynolds and Weber numbers, the two should also be related to each other. In reference 5, the expression

$$\frac{D_m}{D_o} = 22.3\left(\frac{We^*}{Re^*}\right)^{0.29}$$

was obtained. For that case, the Weber number was evaluated as $\sigma/\rho_g D_o V_g^2$, which is actually the reciprocal of the more commonly used Weber number. Also, in reference 5, $Re^* = Re_l(V_g/V_l)$; therefore, for this study, the equation becomes

$$\frac{D_m}{D_o} = 22.3\left[WeRe\left(\frac{V_g}{V_l}\right)\right]^{-0.29} \tag{6}$$

By combining equations (5) and (6), the following relation between the maximum penetration distance and the maximum drop diameter was obtained.

$$\frac{x_m}{D_m} = 0.08\,ReWe^{-0.41}\left(\frac{V_g}{V_l}\right)^{0.29} \tag{7}$$

The plot of equation (7) is shown in figure 8 and the agreement is fairly good.

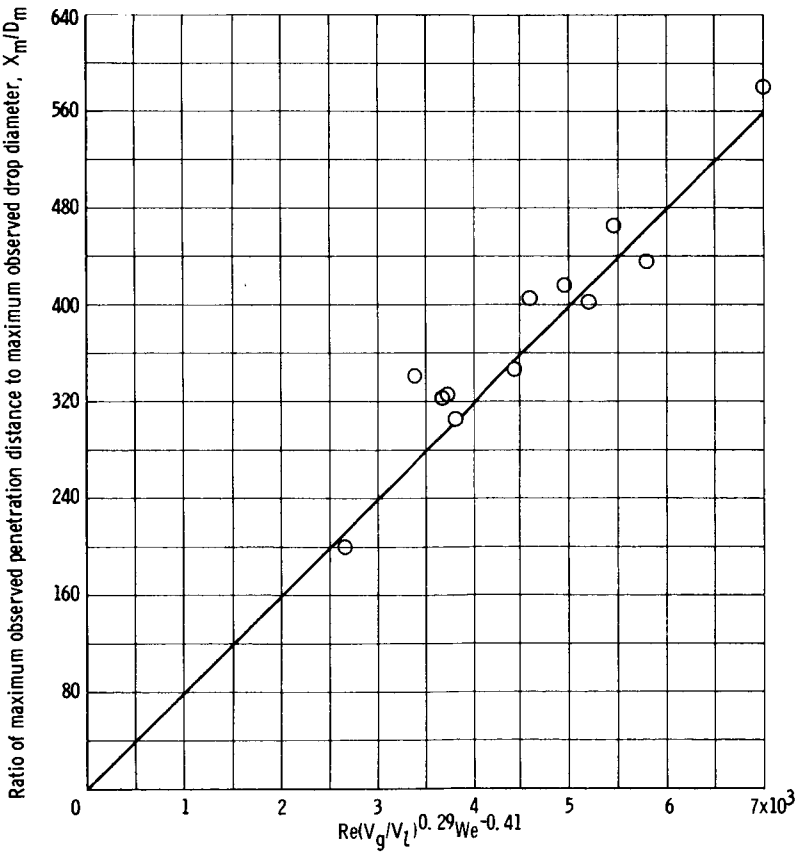

Figure 8. - Relation of maximum penetration distance to maximum drop diameter.

Relation of Point of Maximum Fuel Concentration to Ratio of Reynolds Number and Weber Number

It might be assumed that the point of maximum fuel concentration of the spray X_c is also related to the Reynolds number - Weber number ratio as follows

$$\frac{X_c}{D_o} = f\left(\frac{Re}{We}\right) \tag{8}$$

or,

$$\frac{X_c}{D_o} = b\left(\frac{Re}{We}\right)^p \tag{9}$$

where b and p are constants. From the plot of equation (9), shown in figure 9, it is evident that $X_c/D_o \propto (Re/We)^{0.6}$. Thus, the ratio X_c/D_o was plotted against $(Re/We)^{0.6}$, as shown in figure 10, and equation (9) becomes

$$\frac{X_c}{D_o} = 2.2\left(\frac{Re}{We}\right)^{0.6} \tag{10}$$

which gives the relation of the point of maximum fuel concentration to the Reynolds number - Weber number ratio.

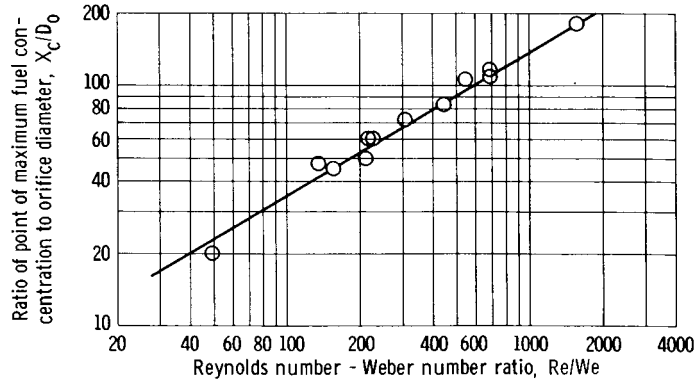

Figure 9. - Effect of Reynolds number - Weber number ratio on point of maximum fuel concentration.

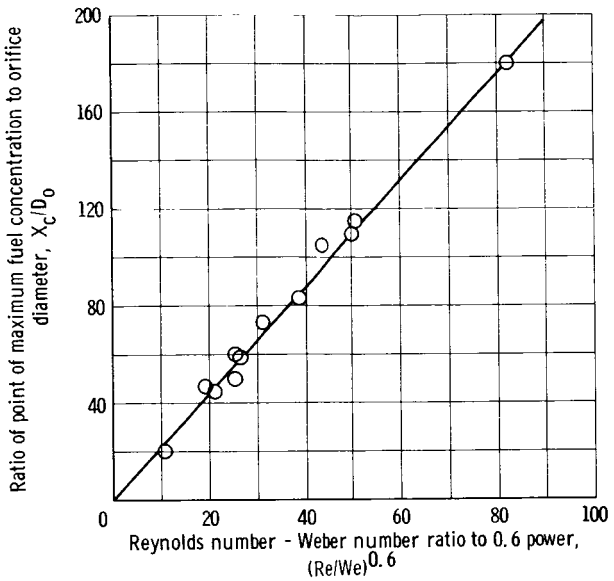

Figure 10. - Evaluation of constant b in equation (9).

Relation of Point of Maximum Fuel Concentration to Volume-Number Mean Drop Diameter

Since the volume-number mean drop diameter D_{30} is also related to the Reynolds and Weber numbers, a relation between it and the point of maximum fuel concentration was investigated. In reference 5, the following expression was derived

$$\frac{D_{30}}{D_o} = 3.9\left(\frac{We^*}{Re^*}\right)^{0.25} \tag{11a}$$

or

$$\frac{D_{30}}{D_o} = 3.9\left[WeRe\left(\frac{V_g}{V_l}\right)\right]^{-0.25} \tag{11b}$$

when the Weber and Reynolds numbers are defined according to their use in this investigation.

Combining equations (10) and (11b) results in the following expression

$$\frac{X_c}{D_{30}} = 0.57\ Re^{0.85}We^{-0.35}\left(\frac{V_g}{V_l}\right)^{0.25} \tag{12}$$

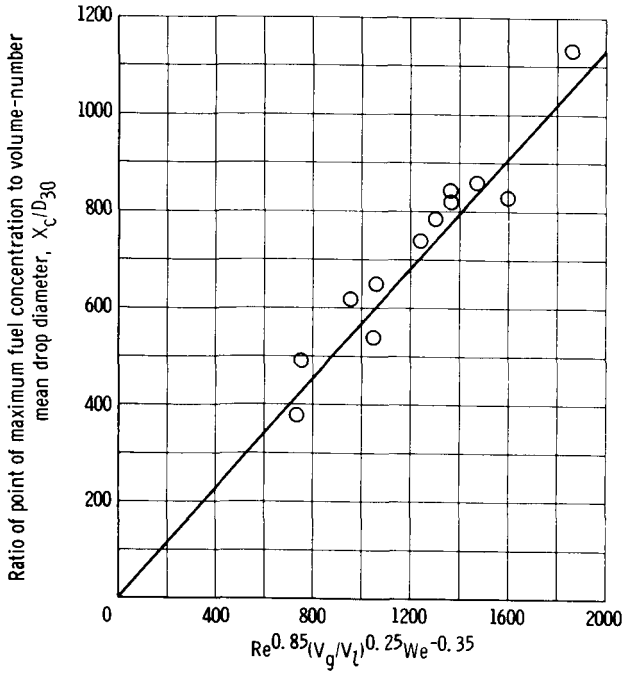

Figure 11. - Relation between point of maximum fuel concentration and volume-number mean drop diameter.

which is plotted in figure 11. Thus, equation (12) gives the relation between the point of maximum fuel concentration and the volume-number mean drop diameter.

Comparison of Results with Chelko's Equation

Maximum penetration distances for water jets injected into airstreams with velocities of 730 to 754 feet per second were determined by Chelko (ref. 6), and the following expression was obtained

$$\frac{x_m}{D_j} = k\left(\frac{V_j}{V_g}\right)^{0.95}\left(\frac{\rho_j}{\rho_g}\right)^{0.74}\left(\frac{s}{D_j}\right)^{0.22} \tag{13}$$

where the constant k is either 0.450 or 0.535; D_j, V_j, and ρ_j are the diameter, velocity, and density, respectively, of the liquid jet; the distance downstream from the orifice is s; and V_g and ρ_g are the velocity and density, respectively, of the airstream.

Values calculated from equation (13) are recorded in table I. The values appear to be somewhat low, particularly at low airstream velocities, when compared with experimental values of x_m. The reason for this can be shown best by a comparison of equation (13) with equation (5) as given in table II. The airstream velocity has exponents of

TABLE II. - COMPARISON OF EQUATION (5) WITH CHELKO'S EQUATION (EQ. (13))

Source	Orifice diameter, D_o, in.	Airstream velocity, V_g, ft/sec	Gas density, ρ_g, lb/ft^3	Liquid velocity, V_l, ft/sec	Liquid density, ρ_l, lb/ft^3	Surface tension, σ, dyne/cm	Liquid viscosity, μ_l, millipoise
Range of variables							
Experimental data	0.010 to 0.040	100 to 300	0.048 to 0.071	51 to 204	42.6	20.7	4.75
Chelko's data	0.0135 to 0.0625	730 to 754	0.082 to 0.133	168 to 229	62	71	10.1
Equation (5)	0.010 to 0.0625	100 to 754	0.048 to 0.133	51 to 229	42.6 to 62	20.7 to 71	4.75 to 10.1
Exponent for Variable							
Chelko's equation	0.78	-0.95	-0.74	0.95	0.74	0	0
Equation (5)	1.0	-1.4	-.7	.7	.7	.7	-.7

-0.95 and -1.4 in equations (13) and (5), respectively. This may be attributed to the fact that the airstream velocity was not varied appreciably in deriving equation (13).

CONCLUSIONS

Maximum penetration distances for crosscurrent injection of isooctane and water jets into airstreams varied directly with the Reynolds number - Weber number ratio as given by the following expression

$$\frac{x_m}{D_o} = 1.8\left(\frac{Re}{We}\right)^{0.7}$$

or

$$\frac{x_m}{D_o} = 1.8\left(\frac{q_l}{q_g}\frac{\sigma}{\mu_l V_l}\right)^{0.7}$$

where x_m is the maximum observed penetration distance, D_o the orifice diameter, Re the Reynolds number, We the Weber number, $q_l = \frac{1}{2}\rho_l V_l^2$ and $q_g = \frac{1}{2}\rho_g V_g^2$, σ is surface tension, μ is viscosity, and V_l is liquid velocity. Similarly, the point of maximum liquid concentration in isooctane sprays was determined by the Reynolds number - Weber number ratio as follows

$$\frac{X_c}{D_o} = 2.2\left(\frac{Re}{We}\right)^{0.6}$$

where X_c is the point of maximum fuel concentration. For isooctane sprays, the ratio of the maximum penetration distance to the maximum drop diameter was correlated with dimensionless groups to give the following expression

$$\frac{x_m}{D_m} = 0.08\ ReWe^{-0.41}\left(\frac{V_g}{V_l}\right)^{0.29}$$

where D_m is the maximum observed drop diameter. Similarly, the following expression was derived for the ratio of the point of maximum fuel concentration in isooctane sprays to the volume-number mean drop diameter:

$$\frac{X_c}{D_{30}} = 0.57\ Re^{0.85}We^{-0.35}\left(\frac{V_g}{V_l}\right)^{0.25}$$

Experimental data obtained in this study and the data obtained by Chelko gave good agreement over a relatively wide range of variables in deriving the preceding expressions. Also, the equation derived by Chelko gave maximum penetration distances that were somewhat lower than those observed for low airstream velocity conditions.

Lewis Research Center
National Aeronautics and Space Administration
Cleveland, Ohio, November 3, 1966
128-31-06-02-22.

REFERENCES

1. Sharp, J. G.: Effects of Fuel Type on the Performance of Aero Gas Turbine Combustion Chambers, and the Influence of Design Features. Roy. Aeron. Soc. J., vol. 58, no. 528, Dec. 1954, pp. 813-825.

2. Staff of the National Gas Turbine Establishment: The Correlation of Combustion Efficiency and Injector Characteristics Under Simulated Altitude Idling Conditions. Combustion Researches and Reviews, NATO-AGARD, Butterworths Scientific Publ. (London), 1955, pp. 53-57.

3. Ingebo, Robert D.: Vaporization Rates and Drag Coefficients for Isooctane Sprays in Turbulent Air Streams. NACA TN 3265, 1954.

4. Foster, Hampton H.; and Ingebo, Robert D.: Evaporation of JP-5 Fuel Sprays in Airstreams. NACA RM E55KO2, 1956.

5. Ingebo, Robert D.; and Foster, Hampton, H.: Drop-Size Distribution for Cross-current Breakup of Liquid Jets in Airstreams. NACA TN 4087, 1957.

6. Chelko, Louis J.: Penetration of Liquid Jets into a High-Velocity Air-Stream. NACA RM E50F21, 1950.

NASA-Langley, 1967 —— 12 E-3664